HETEROCYCLES, Vol. 106, No. 8, 2023, pp. 1315 - 1333. © 2023 The Japan Institute of Heterocyclic Chemistry
Received, 23rd May, 2023, Accepted, 22nd June, 2023, Published online, 28th June, 2023
DOI: 10.3987/COM-23-14869

DESIGN, SYNTHESIS, AND BIOLOGICAL EVALUATION OF 4*H*-PYRIDO[1,2-*a*]PYRIMIDIN-4-ONE DERIVATIVES AS ANTICANCER AGENTS VIA ROR1 INHIBITION

Mei-Tao Yuan,[1,2] Xin-Ran Zhao,[2,3] Liang Xiong,[2,3] Ting Zhong,[2,3] Fang Luo,[2,3] Qing Li,[2,3] Mei Li,[2,3] Hong-Shan Wu,[2,3] Ai-Ling Linghu,[2,3] Xiao-Sheng Yang,[1,2]* and Yan-Hua Fan[2,3]*

[1] School of Pharmacy, Guizhou University, Guiyang 550025, PR China.
[2] The Key Laboratory of Chemistry for Natural Products of Guizhou Province and Chinese Academy of Sciences, Guiyang 550014, PR China.
[3] State Key Laboratory for Functions and Applications of Medicinal Plants, Guizhou Medical University, Guiyang 550014, PR China.
[*] Corresponding author at: State Key Laboratory for Functions and Applications of Medicinal Plants, Guizhou Medical University, Guiyang 550014, PR China. E-mail address: gzcnp@sina.cn (Xiao-Sheng Yang); yhfan@gmc.edu.cn (Yan-Hua Fan).

Abstract – Based on the chroman-4-one ROR1 inhibitor **ARI-1**, two new series of 4*H*-pyrido[1,2-*a*]pyrimidin-4-one derivatives were designed and synthesized, and their biological activities were investigated. *In vitro* biological activity assays showed that compound **10b** exhibited the best antiproliferation activity against H1975 (IC_{50} = 0.572 μM), which was superior to the lead compound **ARI-1** (IC_{50} = 3.51 μM). Compound **10b** also dose-dependently induced G0/G1 phase block and apoptosis. In addition, **10b** exhibited inhibitory activity against ROR1 and modulated the ROR1 signaling pathway in a dose-dependent manner to exert anticancer activity. In conclusion, our data suggest that **10b** may be a new lead compound for further development of ROR1 inhibitors as anti-cancer agents.

INTRODUCTION

Lung cancer remains the leading cause of cancer deaths worldwide, and it also has a low 5-year survival rate of only 18%.[1] The main types of lung cancer are divided into non-small cell lung cancer (NSCLC) and small cell lung cancer (SCLC), with the proportion of NSCLC accounting for 80-90% of all lung

cancers. Lung adenocarcinoma is the most common type of NSCLC and has one of the highest mortality rates.[2] Epidermal growth factor receptor tyrosine kinase inhibitors (EGFR-TKIs) are indeed effective in the treatment of NSCLC, but most patients inevitably develop acquired resistance after 8-10 months.[3] Although third-generation EGFR-TKIs (Osimertinib) have partially solved the problem of drug resistance, there are still many patients who cannot receive effective treatment.[4] Therefore, it is important to develop new targeted inhibitors for the treatment of lung cancer.

Receptor tyrosine kinase-like orphan receptor 1 (ROR1) is expressed at very low levels in normal and differentiated mature tissues, but is over-expressed in various cancers and is associated with cancer cell proliferation, survival and metastasis.[5] Therefore, ROR1 is considered as a potential target for the development of antitumor drugs. Due to the early discovery of negligible catalytic activity of ROR1 *in vitro*, the development of small molecule inhibitors of ROR1 lagged far behind its monoclonal antibodies.[6] As research has progressed, ROR1 has been shown to undergo tyrosine phosphorylation, which allows ROR1 to have kinase activity in vivo, thus providing a theoretical basis for the development of small molecule inhibitors.[7] However, only a few small molecule inhibitors of ROR1 have been reported. Therefore, it is important to develop more small-molecule inhibitors of ROR1 to better exploit its potential in cancer therapy.

Chroman-4-one is a class of six-membered heterocyclic compounds (Figure 1). It is a special component in drug design and discovery, which is widely distributed in nature and has various biological activities such as potential anticancer, antitubercular and antibacterial.[8] Among them, chroman-4-one derivative **ARI-1** was found to exert anticancer effects by inhibiting the expression of ROR1, which exhibited the best antiproliferation activity against human non-small cell lung adenocarcinoma cells H1975 cells with the half maximum inhibitory concentration value (IC_{50}) of 3.51 μM. Their studies suggested that **ARI-1** was an attractive drug candidate in the treatment of NSCLC.[9]

Therefore, as shown in Figure 1, we used **ARI-1** as the lead compound and replaced its chroman-4-one structure with 4*H*-pyrido[1,2-*a*]pyrimidin-4-one using a scaffold hopping method. At the same time, we considered the introduction of arylurea structures because they have various biological activities such as anticancer.[10] In addition, the benzimidazole structure is also a potent moiety for anticancer drugs, and a series of compounds with anticancer activity were synthesized in our previous work.[11] Based on these findings, in the present study, we designed and synthesized 17 compounds of 4*H*-pyrido[1,2-*a*]pyrimidin-4-one and evaluated the anticancer activity of these compounds. *In vitro* antiproliferation activity assays showed that compound **10b** exhibited the best antiproliferation activity against H1975 tumor cells (IC_{50} = 0.572 μM), and the effect of **10b** on ROR1 and its downstream pathways was also further evaluated.

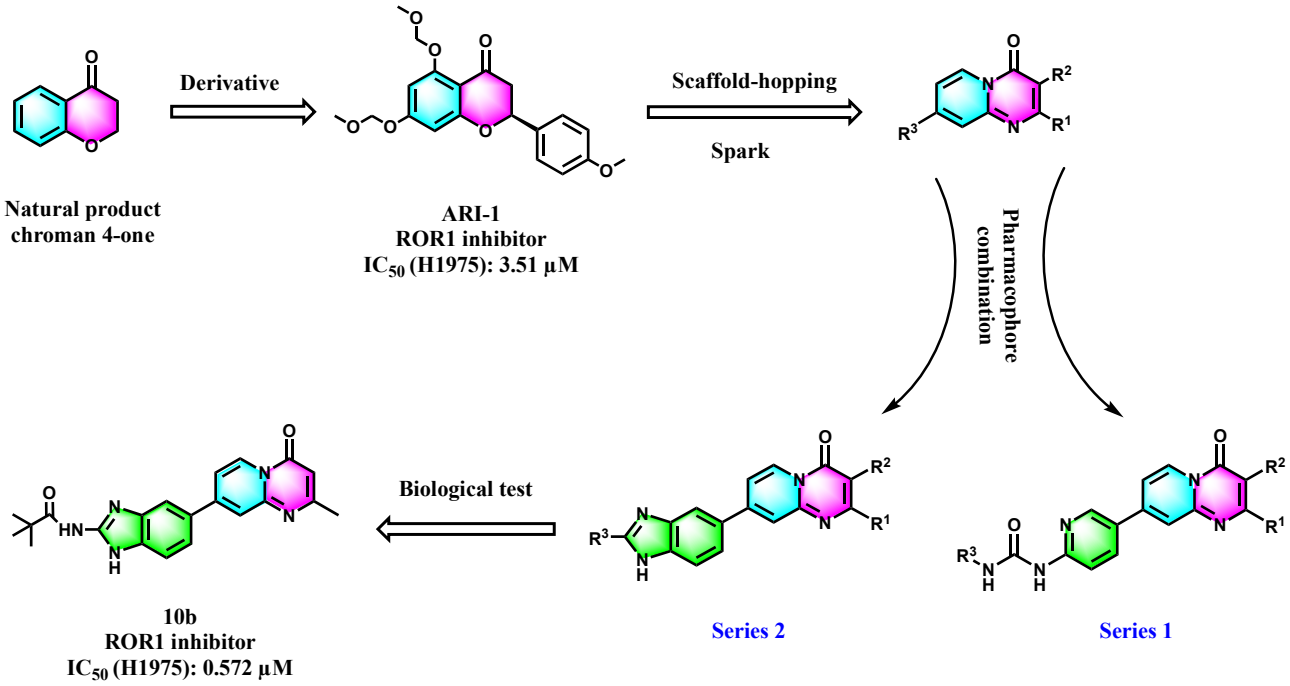

Figure 1. Design strategies for target compounds

RESULTS AND DISCUSSION

Chemical synthesis. Scheme 1 describes the synthesis of the target compounds **4a-n** as series 1. First, intermediate **2a** was synthesized from 4-bromo-2-aminopyridine with substituted β-keto esters according to a previous study.[12] Then, 2-aminopyridine-5-boronic acid pinacol ester (**2b**) was subjected to Suzuki-Miyaura cross-coupling reaction with intermediate **2a** to give intermediate **3**. Finally, **3** was reacted with differently substituted phenyl isocyanates to give the target products **4a-n**.

Scheme 2 describes the synthesis of the target compounds **10a-c** as series 2. 4-Bromo-2-nitroaniline **5** was treated with bis(pinacolato)ethylborane to give **6**. Then, intermediates **6** and **2a** (synthesized in Scheme 1) were used as the main raw materials, and intermediates **7**-**9** and target compounds **10a-c** were synthesized by a series of well-established reactions such as Suzuki-Miyaura cross-coupling, reduction, cyclization and acylation, respectively, and purified by through column chromatography separation.

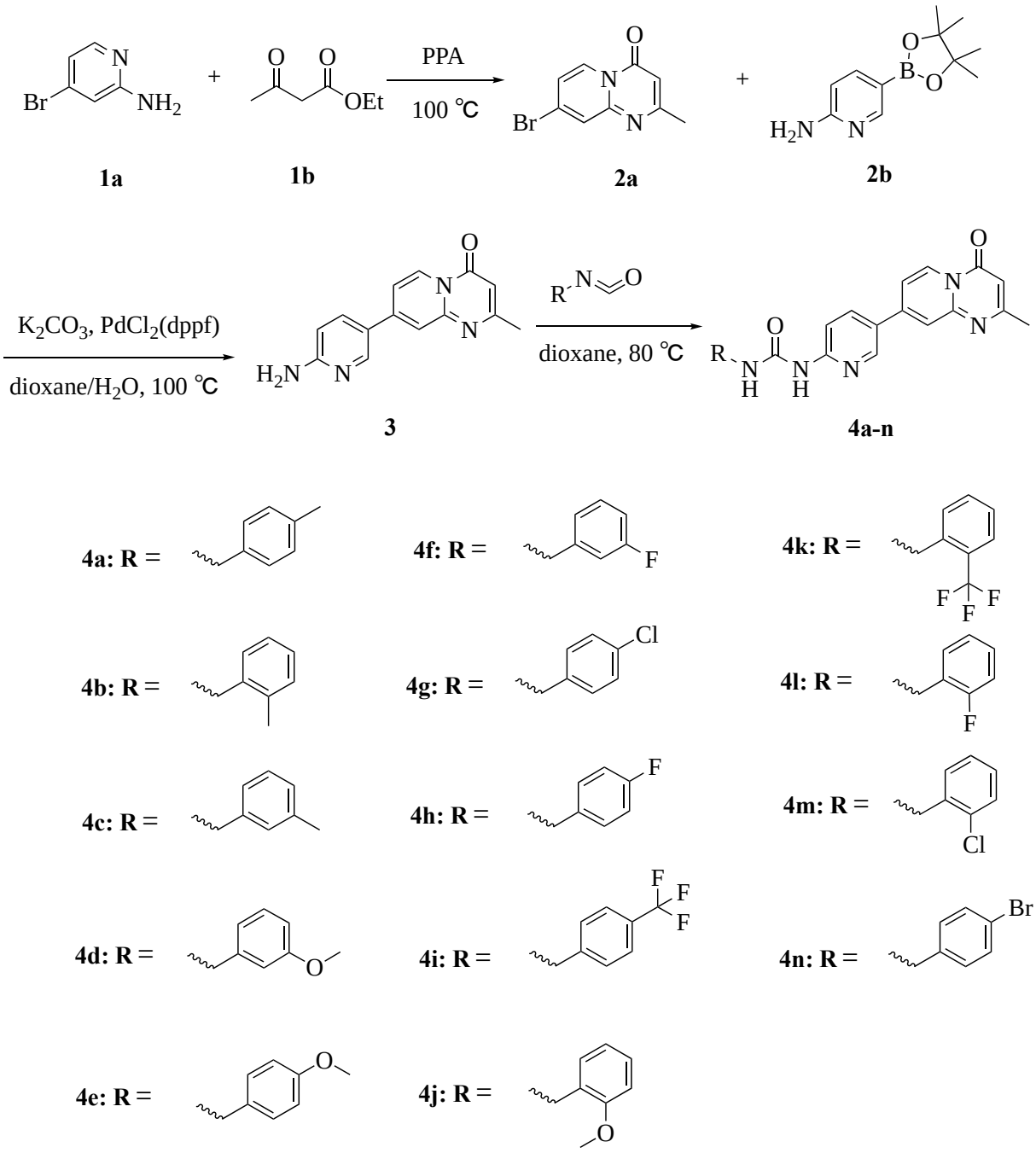

Scheme 1. Synthetic route of compounds **4a-n**

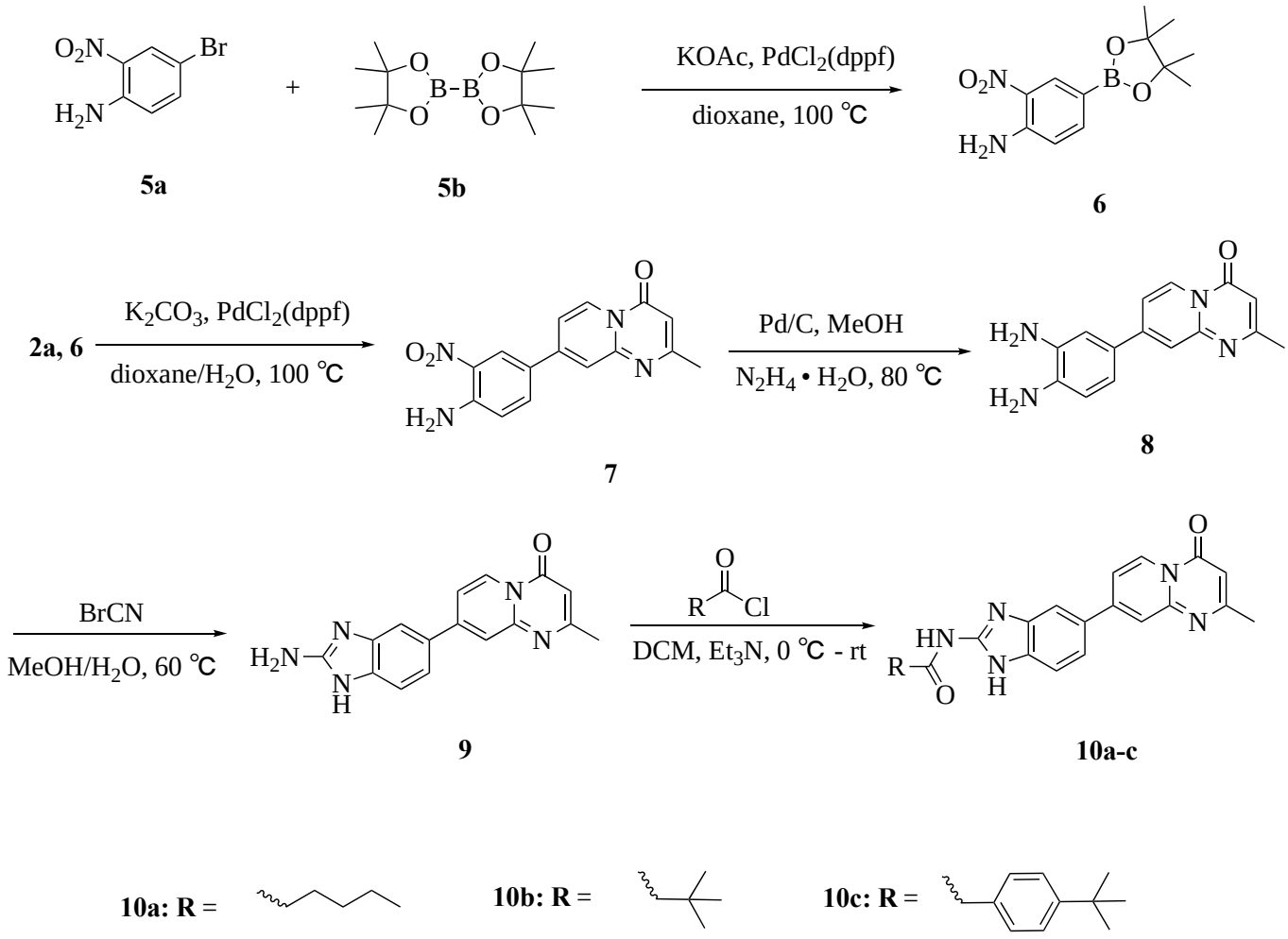

Scheme 2. Synthetic route of compounds **10a-c**

Antiproliferation activity assay. Table 1 shows that compounds **4a-n** did not exhibit antiproliferation activity, suggesting that the introduction of the pyridin-2-amine portion at the C-8 position of 4*H*-pyrido[1,2-*a*]pyrimidin-4-one is unfavorable. However, the introduction of the benzimidazole structure seems to be beneficial for the compounds to exert antiproliferation activity. This series of compound **10b** showed the best antiproliferation ability against H1975 cells in the tested lung cancer cell lines with an IC_{50} value of 0.572 μM, which is nearly 6-fold higher than its lead compound **ARI-1**. Therefore, **10b** was selected for further mechanistic studies.

Table 1. Antiproliferation activity of 17 compounds in different cells (IC_{50}, μM)

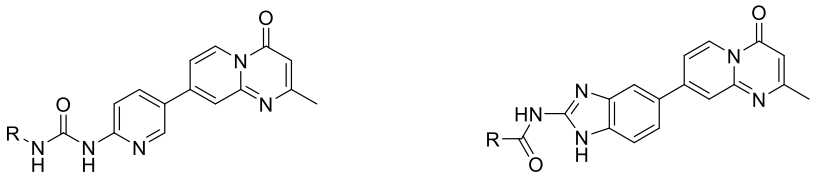

4a-n (Series 1) **10a-c** (Series 2)

Comp.	R	Antiproliferation Activity IC_{50} ±SD (μM)[a]		
		PC-9	H1975	A549/T
4a	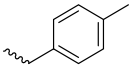	＞20	＞20	＞20
4b	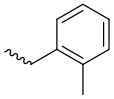	＞20	＞20	18.85±0.643
4c	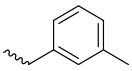	＞20	＞20	＞20
4d	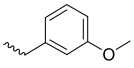	＞20	＞20	＞20
4e	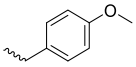	＞20	＞20	＞20
4f	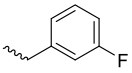	＞20	＞20	＞20
4g	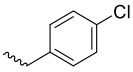	＞20	＞20	＞20
4h	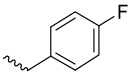	＞20	＞20	＞20
4i	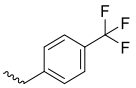	＞20	＞20	＞20
4j	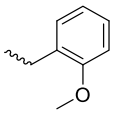	＞20	＞20	＞20
4k	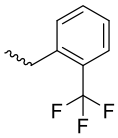	＞20	＞20	＞20
4l	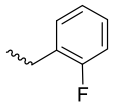	＞20	＞20	＞20
4m	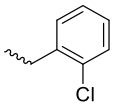	＞20	＞20	＞20
4n	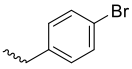	＞20	＞20	＞20
10a	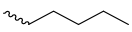	＞20	＞20	＞20
10b		＞20	**0.572±0.040**	1.36±0.297
10c	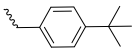	16.985±0.247	8.66±0.260	6.529±0.084

[a] Data are expressed as mean ± SD from three different experiments.

Effect of 10b on the cell cycle. A significant G0/G1 phase block was observed in cells treated with **10b** (1.25 μM and 2.5 μM) for 48 h compared to the control (the percentage of G1 phase cells increased from 46.30% to 57.05%). When the concentration was increased to 5 μM, the percentage of cells in G0/G1 phase decreased with a corresponding increase in cells in sub-G1 phase, indicating that the cells would

eventually apoptosis or die due to cycle arrest (Figure 2, **A**). The results indicated that compound **10b** inhibited the growth and proliferation of H1975 cells by inducing G0/G1 phase block. Meanwhile, the expression of cell cycle regulatory proteins was determined by western blot analysis. It was observed that the expression levels of cell cycle protein B1 and CDK1 were also reduced after treatment with **10b** (Figure 2, **B-D**).

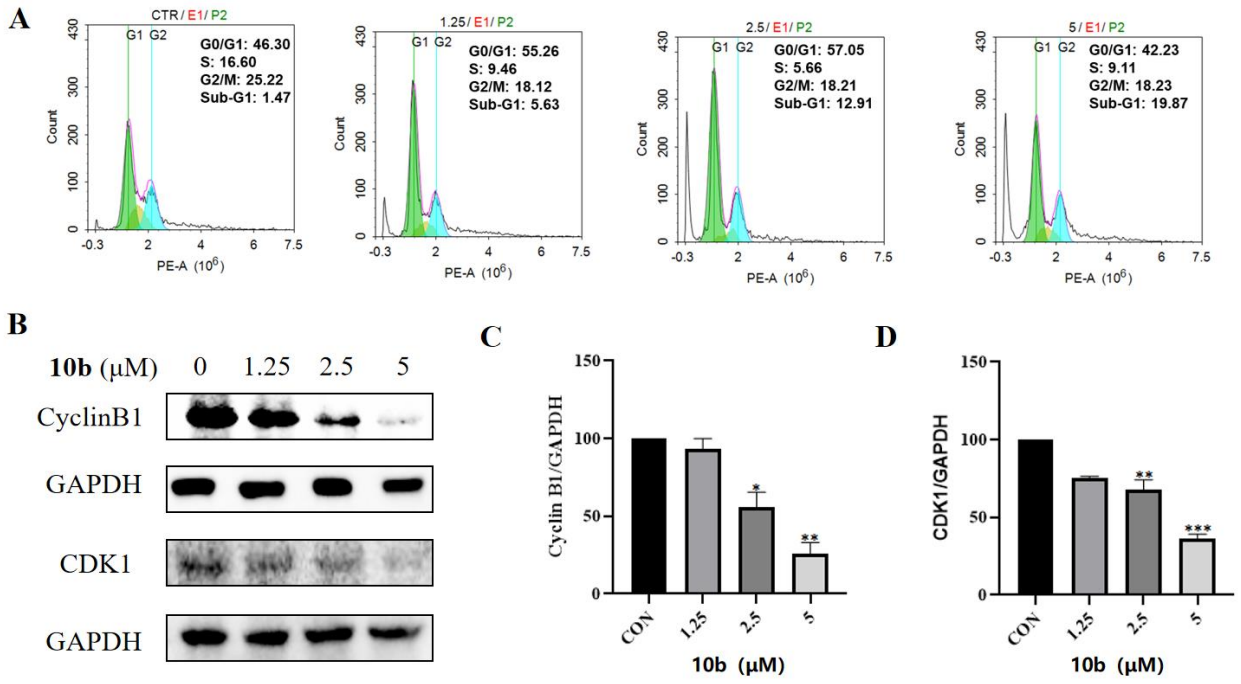

Figure 2. Effect of compound **10b** on H1975 cell cycle (**A**) and western blot analysis of cell cycle-associated protein expression (**B-D**). Each bar data is expressed as mean ± SD from two parallel experiments (*p < 0.05, **p < 0.01, ***P < 0.001 vs. control).

Effect of 10b on cell apoptosis. Cells treated with **10b** induced apoptosis in a dose-dependent manner compared with the control group (Figure 3, **A**). To further elucidate the potential mechanism of apoptosis induction by **10b**, the effect of **10b** on the expression levels of apoptosis-related proteins was examined by western blot. The pro-apoptotic proteins cleaved-caspase 3 and cleaved-caspase 9 were up-regulated in a concentration-dependent manner after **10b** treatment compared to the control (Figure 3, **B-D**). These results suggest that compound **10b** induced apoptosis in H1975 cells in a concentration-dependent manner.

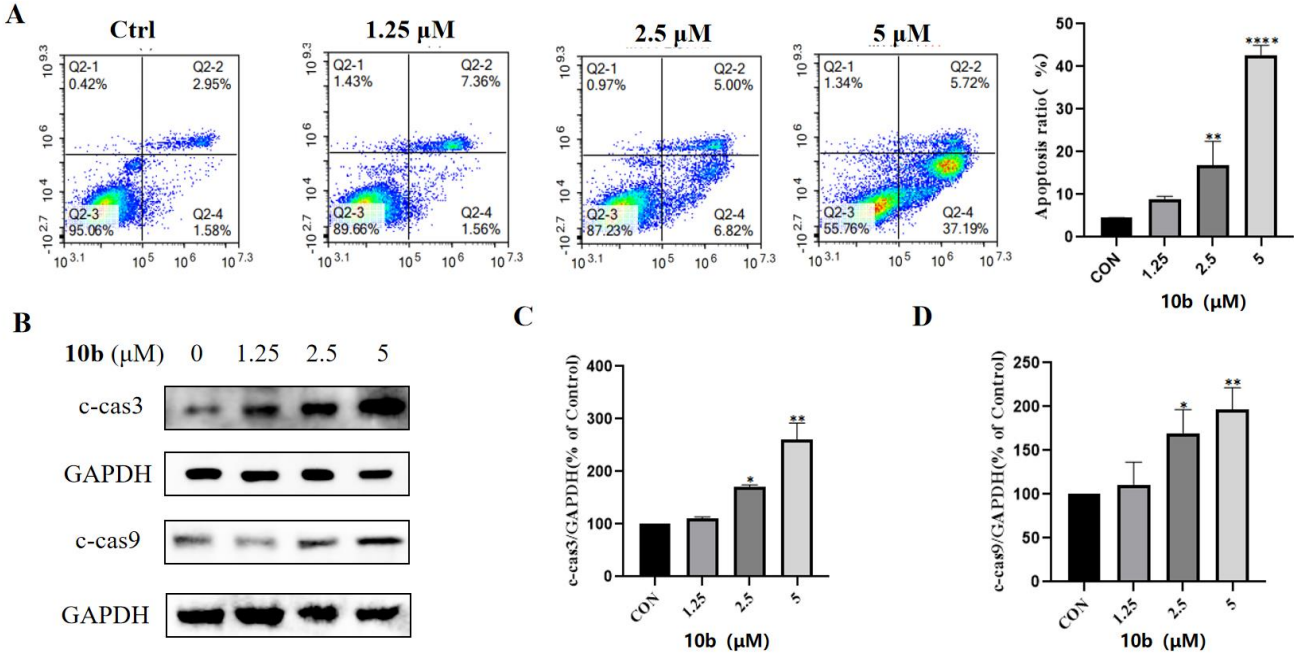

Figure 3. Effect of compound **10b** on apoptosis of H1975 cells (**A**) and western blot analysis of apoptosis-associated proteins (**B-D**). GAPDH was used as a loading control. Each bar data is expressed as the mean ± SD of two parallel experiments (*p<0.05, **p<0.01, ***p<0.0001 vs. control).

Effect of 10b on ROR1 signaling pathway. Due to the ROR1 inhibitory activity of the lead compound **ARI-1** and the previous finding that the catalytic activity of ROR1 is negligible *in vitro*,[6] we were unable to test the kinase inhibitory activity of **10b** *in vitro*. In addition, it was shown that the tyrosine kinase Lyn can phosphorylate multiple tyrosine sites in the intracellular structural domain of ROR1, which contributes to the recruitment of the ubiquitin E3 ligase c-CBL, thereby degrading ROR1.[13] Herein, we will focus on investigate the effects of **10b** on the protein levels of ROR1 and p-ROR1, as well as the activation of its downstream signaling pathways.

Treatment of H1975 cells with **10b** for 48 h resulted in increased expression of p-ROR1, which is consistent with previous findings. In contrast, the total protein of ROR1 was reduced, indicating that ROR1 was inhibited by **10b** (Figure 4, **A**). In **10b**-treated cells, the ROR1-controlled downstream ASK1/P38 pro-apoptotic pathway was reactivated with increased p-P38, thereby promoting apoptosis (Figure 4, **B**). In addition, the Akt/GSK-3β/mTOR pathway is one of the important pro-survival signals of the ROR1/Src pathway and is involved in tumor cell development.[14] Experimental results showed that treatment of cells with **10b** resulted in a significant decrease in phosphorylation of Src, Akt, mTOR and GSK3β, indicating that **10b** inhibited Akt/GSK-3β/mTOR signaling. In conclusion, these data suggest that compound **10b** can inhibit the proliferation and induce apoptosis in H1975 tumor cells by inhibiting ROR1 and its downstream Src/Akt signaling pathway and activating ASK1/P38 pro-apoptotic pathway.

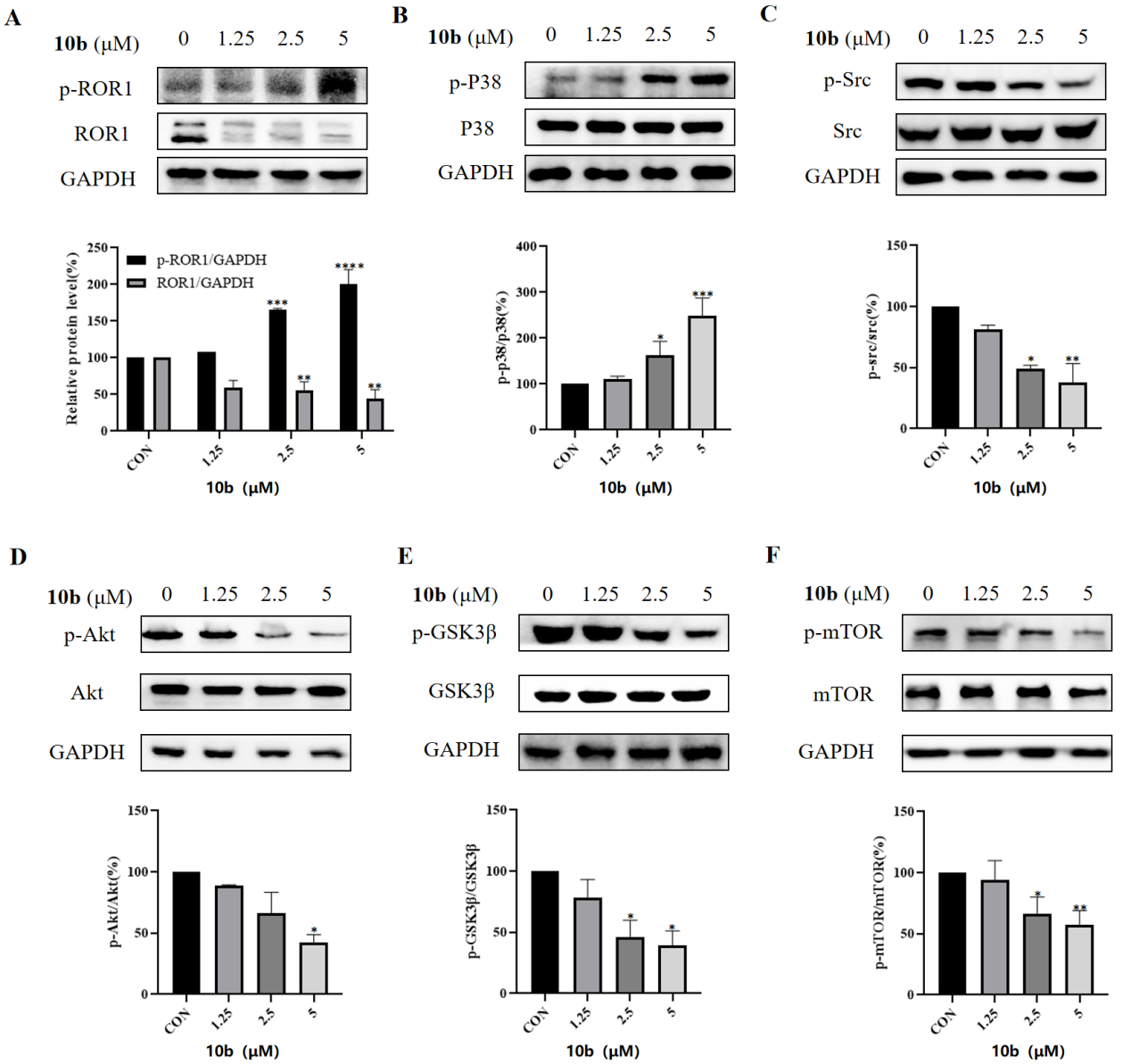

Figure 4. Compound **10b** inhibits the expression of ROR1 (**A**) and its downstream associated proteins (**B-F**). Each bar data is expressed as the mean ± SD of two parallel experiments (*p<0.05, **p<0.01, ***p<0.001, ***p<0.0001 vs. control).

Molecular docking. We analyzed the binding pattern of **10b** and ROR1 (PDB code: 6TU9) by molecular docking simulations. The results showed that the binding pattern of **10b** was similar to that of the previously identified ROR1 inhibitor, **10b** formed two hydrogen bonds with residues Ile55 and Asp633, and pi-pi stacking interaction with Phe552 was also observed. Meanwhile, **10b** can form a salt bridge with residue Glu523. In addition, van der Waals and alkylated hydrophobic interactions including pi alkyl also contribute to the stable binding between **10b** and ROR1 (Figure 5).

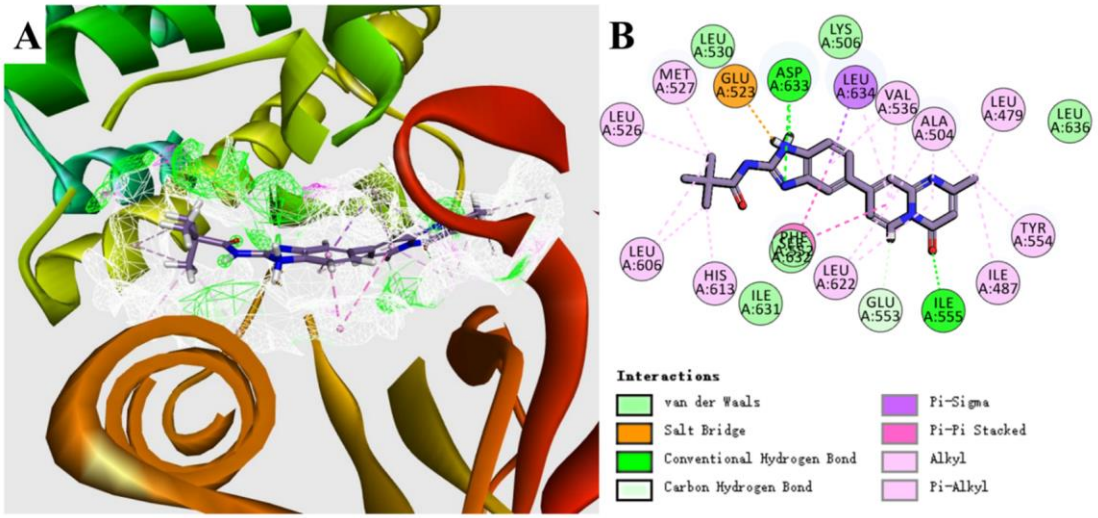

Figure 5. Molecular docking study of **10b** with ROR1 (PDB code 6TU9)

In summary, 17 compounds were designed and synthesized by scaffold hopping strategy for the chroman-4-one derivative **ARI-1**, combined with the pharmacophore of known anticancer drugs. *In vitro* antiproliferation assays showed that compound **10b** exhibited the best antiproliferation activity against H1975 cells with an IC_{50} value of 0.572 μM, which was nearly 6-fold better than the lead compound **ARI-1**. In addition, preliminary mechanistic studies showed that compound **10b** could inhibit cell proliferation and induce apoptosis by inhibiting ROR1 and its down-regulated signaling pathway. In conclusion, our study provides a new attractive lead compound for further development of novel ROR1 inhibitors, and more ROR1 inhibitors as anticancer drugs are expected to be developed based on this study.

EXPERIMENTAL

The raw materials and solvents used for the experiments were commercially available and used directly without purification. All reactions were monitored by thin layer chromatography (TLC). High resolution precision mass is measured on a quadrupole time of flight (QTOF) mass spectrometer (micro TOF-Q, Bruker Inc.) using electrospray ionization (positive mode). ^{1}H NMR, ^{13}C NMR and ^{19}F NMR spectral data were recorded by 600, 150 and 565 MHz Bruker AVANCE NEO NMR spectrometer, respectively, and analyzed using MestReNova 14.2 as processing software. The spectra were recorded at 25 °C and measured using DMSO-d_6 and tetramethylsilane (TMS) as solvent and internal standard, respectively. All chemical shifts (d) are in ppm and the coupling constants (J) are in Hz. Infrared spectral data of the compounds were determined by FTIR spectrometer. The purity of the active compound **10b** was determined by AgilentLC1260 liquid chromatography. The melting points of all target compounds were determined using a Shanghai micro melting point meter.

General procedure for the preparation of 4. (5-(2-Methyl-4-oxo-4*H*-pyrido[1,2-*a*]pyrimidin-8-yl)-pyridin-2-yl)-3-(*p*-tolyl)urea (4a). First, intermediate **2a** was synthesized according to the method described in the literature.[12] That is, 4-bromo-2-aminopyridine (2.59 g, 15 mmol) was mixed with ethyl 3-oxobutanoate (2.93 g, 22.5 mmol) under argon, then polyphosphoric acid (PPA) was added and heated to 100 °C for stirring. After 2 h, the mixture was cooled to room temperature and the pH was adjusted to neutral with 5% aqueous sodium hydroxide in an ice bath environment, filtered and washed with water. The solid precipitate was collected to obtain the crude product. The filtrate was extracted with dichloromethane (DCM), the organic phase was concentrated and the crude product was purified by column chromatography to give a white solid intermediate **2a** (2.18 g, 9.16 mmol, 61.1% yield).

Then, intermediate **2a** (1.19 g, 5 mmol), 2-aminopyridine-5-boronic acid pinacol ester (1.10 g, 5 mmol), K_2CO_3 (2.07 g, 15 mmol) and $Pd(dppf)Cl_2$ (0.18 g, 0.25 mmol) were added to 30 mL of 1,4-dioxane/water solvent ($V_{dioxane}$: V_{water} = 4:1), excluding oxygen, heated to 100 °C and stirred at reflux for 4-5 h. The solvent was removed under reduced pressure and the residue was purified by column chromatography using DCM/methanol (MeOH) as mobile phase to give 8-(6-aminopyridin-3-yl)-2-methyl-4*H*-pyrido[1,2-*a*]pyrimidin-4-one (**3**) as a yellow solid (0.89 g, 3.53 mmol, 70.6% yield). ^{1}H NMR (600 MHz, DMSO-d_6) δ 8.83 (d, *J* = 7.5 Hz, 1H), 8.59 (d, *J* = 2.6 Hz, 1H), 8.01 (dd, *J* = 8.8, 2.7 Hz, 1H), 7.78 (d, *J* = 2.1 Hz, 1H), 7.67 (dd, *J* = 7.6, 2.1 Hz, 1H), 6.61 (s, 2H), 6.57 (d, *J* = 8.7 Hz, 1H), 6.17 (s, 1H), 2.33 (s, 3H); ^{13}C NMR (150 MHz, DMSO-d_6) δ 165.22, 161.10, 156.94, 150.95, 147.87, 145.83, 135.65, 126.95, 118.49, 117.16, 113.27, 108.29, 101.04, 24.25; FT-IR (KBr, cm^{-1}): 1635.43 (stretch C=O), 3432.91 (stretch -NH_2); MS (ESI): *m/z* 251.1 $[M-H]^-$; HRMS (ESI): $C_{14}H_{13}N_4O$ ($[M+H]^+$): calcd 253.1084, found 253.1075.

Finally, intermediate **3** (0.25 g, 1 mmol) was mixed with *p*-toluene isocyanate (0.40 g, 3 mmol) and was added to 20 mL of 1,4-dioxane solvent, oxygen was excluded, the temperature was raised to 80 °C and stirred for 4-9 h. After completion of the reaction, the solvent was removed by concentration under reduced pressure and the residue was purified by column chromatography on silica gel using DCM/MeOH to give **4a** (0.28 mg, 72.6%); white solid; mp >270 °C; ^{1}H NMR (600 MHz, DMSO-d_6) δ 10.14 (s, 1H), 9.66 (s, 1H), 8.92 – 8.89 (m, 2H), 8.36 (dd, *J* = 8.9, 2.6 Hz, 1H), 7.96 (d, *J* = 2.1 Hz, 1H), 7.73 (dd, *J* = 7.6, 2.1 Hz, 1H), 7.70 (d, *J* = 8.8 Hz, 1H), 7.40 (d, *J* = 8.0 Hz, 2H), 7.12 (d, *J* = 7.9 Hz, 2H), 6.25 (s, 1H), 2.37 (s, 3H), 2.26 (s, 3H); ^{13}C NMR (150 MHz, DMSO-d_6) δ 165.62, 157.25, 154.50, 152.31, 151.08, 146.73, 144.92, 137.47, 136.65, 132.13, 129.78, 127.73, 124.85, 120.27, 119.35, 113.99, 112.31, 102.25, 24.59, 20.84; FT-IR (KBr, cm^{-1}): 1693.28 (stretch C=O), 1515.03 (bending N-H and stretch C-N), 3429.45 (stretch N-H); MS (ESI): *m/z* 384.1 $[M-H]^-$; HRMS (ESI): $C_{22}H_{20}O_2N_5$ ($[M+H]^+$): calcd 386.1612, found 386.1608.

1-(5-(2-Methyl-4-oxo-4*H*-pyrido[1,2-*a*]pyrimidin-8-yl)pyridin-2-yl)-3-(*o*-tolyl)urea (4b): yellowish solid; 75.3% yield; mp >270 ℃; ^{1}H NMR (600 MHz, DMSO-d_6) δ 10.38 (s, 1H), 9.87 (s, 1H), 8.93 – 8.89 (m, 2H), 8.34 (dd, *J* = 8.7, 2.4 Hz, 1H), 7.98 (d, *J* = 8.1 Hz, 1H), 7.94 (d, *J* = 2.0 Hz, 1H), 7.71 (dd, *J* = 7.5, 2.0 Hz, 1H), 7.56 (d, *J* = 8.8 Hz, 1H), 7.22 (d, *J* = 7.6 Hz, 1H), 7.17 (t, *J* = 7.6 Hz, 1H), 6.99 (t, *J* = 7.6 Hz, 1H), 6.23 (s, 1H), 2.38 (s, 3H), 2.36 (s, 3H); ^{13}C NMR (150 MHz, DMSO-d_6) δ 165.56, 157.21, 154.61, 152.45, 151.09, 146.23, 144.73, 137.61, 137.58, 130.73, 127.68, 127.59, 126.77, 124.61, 123.45, 120.80, 120.35, 113.93, 112.46, 102.26, 24.58, 18.65; FT-IR (KBr, cm^{-1}): 1687.51 (stretch C=O), 1516.04 (bending N-H and stretch C-N), 3432.19 (stretch N-H); MS (ESI): *m/z* 384.1 [M-H]$^-$; HRMS (ESI): $C_{22}H_{20}O_2N_5$ ([M+H]$^+$): calcd 386.1612, found 386.1608.

1-(5-(2-Methyl-4-oxo-4*H*-pyrido[1,2-*a*]pyrimidin-8-yl)pyridin-2-yl)-3-(*p*-tolyl)urea (4c): yellowish solid; 75.3% yield; mp >270 ℃; ^{1}H NMR (600 MHz, DMSO-d_6) δ 10.21 (s, 1H), 9.68 (s, 1H), 8.89 (dd, *J* = 5.1, 2.5 Hz, 2H), 8.35 (dd, *J* = 8.9, 2.6 Hz, 1H), 7.94 (d, *J* = 2.2 Hz, 1H), 7.71 (dd, *J* = 7.5, 2.1 Hz, 1H), 7.68 (d, *J* = 8.8 Hz, 1H), 7.32 (dd, *J* = 10.9, 3.0 Hz, 2H), 7.19 (t, *J* = 7.7 Hz, 1H), 6.84 (d, *J* = 7.4 Hz, 1H), 6.23 (s, 1H), 2.35 (s, 3H), 2.29 (s, 3H); ^{13}C NMR (150 MHz, DMSO-d_6) δ 165.53, 157.18, 154.44, 152.23, 151.04, 146.65, 144.77, 139.18, 138.61, 137.39, 129.20, 127.64, 124.79, 123.87, 120.25, 119.71, 116.39, 113.85, 112.27, 102.23, 24.59, 21.64; FT-IR (KBr, cm^{-1}): 1682.42 (stretch C=O), 1520.43 (bending N-H and stretch C-N), 3439.82 (stretch N-H); MS (ESI): *m/z* 384.1 [M-H]$^-$; HRMS (ESI): $C_{22}H_{20}O_2N_5$ ([M+H]$^+$): calcd for 386.1612, found 386.1610.

1-(3-Methoxyphenyl)-3-(5-(2-methyl-4-oxo-4*H*-pyrido[1,2-*a*]pyrimidin-8-yl)pyridin-2-yl)urea (4d): yellowish solid; 66.3% yield; mp >270 ℃; ^{1}H NMR (600 MHz, DMSO-d_6) δ 10.21 (s, 1H), 9.67 (s, 1H), 8.93 – 8.90 (m, 2H), 8.39 – 8.36 (m, 1H), 7.98 (s, 1H), 7.74 (dd, *J* = 7.9, 2.5 Hz, 2H), 7.24 – 7.21 (m, 2H), 7.02 – 7.00 (m, 1H), 6.62 (dd, *J* = 8.2, 2.5 Hz, 1H), 6.27 – 6.23 (m, 1H), 3.75 (s, 3H), 2.37 (s, 3H); ^{13}C NMR (150 MHz, DMSO-d_6) δ 165.55, 160.20, 157.19, 154.37, 152.21, 151.06, 146.71, 144.81, 140.46, 137.41, 130.15, 127.67, 124.93, 120.29, 113.89, 112.32, 111.54, 108.52, 105.05, 102.24, 55.48, 24.59; FT-IR (KBr, cm^{-1}): 1644.19 (stretch C=O), 1520.49 (bending N-H and stretch C-N), 1248.34 (stretch -O-CH_3 Ar.), 3443.39 (stretch N-H); MS (ESI): *m/z* 400.1 [M-H]$^-$; HRMS (ESI): $C_{22}H_{20}O_3N_5$ ([M+H]$^+$): calcd 402.1561, found 402.1558.

1-(4-Methoxyphenyl)-3-(5-(2-methyl-4-oxo-4*H*-pyrido[1,2-*a*]pyrimidin-8-yl)pyridin-2-yl)urea (4e): yellowish solid; 61.7% yield; mp >270 ℃; ^{1}H NMR (600 MHz, DMSO-d_6) δ 10.07 (s, 1H), 9.62 (s, 1H), 8.90 (d, *J* = 7.5 Hz, 1H), 8.88 (d, *J* = 2.5 Hz, 1H), 8.34 (dd, *J* = 8.8, 2.6 Hz, 1H), 7.95 (d, *J* = 2.0 Hz, 1H), 7.72 (dd, *J* = 7.5, 2.1 Hz, 1H), 7.68 (d, *J* = 8.8 Hz, 1H), 7.42 (d, *J* = 8.9 Hz, 2H), 6.90 (d, *J* = 8.9 Hz, 2H), 6.24 (s, 1H), 3.73 (s, 3H), 2.36 (s, 3H); ^{13}C NMR (150 MHz, DMSO-d_6) δ 165.13, 156.77, 155.06, 154.14, 151.96, 150.64, 146.24, 144.43, 136.94, 131.77, 127.24, 124.28, 120.65, 119.80, 114.11, 113.47, 111.82, 101.79, 29.06, 24.16; FT-IR (KBr, cm^{-1}): 1693.17 (stretch C=O), 1513.73 (bending N-H and stretch C-N),

1240.97 (stretch -O-CH_3 Ar.), 3411.46 (stretch N-H); MS (ESI): *m/z* 400.5 $[M-H]^-$; HRMS (ESI): $C_{22}H_{20}O_3N_5$ ($[M+H]^+$): calcd 402.1561, found 402.1560.

1-(3-Fluorophenyl)-3-(5-(2-methyl-4-oxo-4*H*-pyrido[1,2-*a*]pyrimidin-8-yl)pyridin-2-yl)urea (4f): yellowish solid; 88.9% yield; mp >270 °C; ^{1}H NMR (600 MHz, DMSO-d_6) δ 10.42 (s, 1H), 9.77 (s, 1H), 8.94 – 8.91 (m, 2H), 8.40 (dd, *J* = 8.8, 2.6 Hz, 1H), 7.98 (d, *J* = 2.1 Hz, 1H), 7.76 – 7.73 (m, 2H), 7.58 – 7.54 (m, 1H), 7.37 – 7.33 (m, 1H), 7.20 (dd, *J* = 8.1, 2.0 Hz, 1H), 6.86 (td, *J* = 8.5, 2.6 Hz, 1H), 6.26 (s, 1H), 2.37 (s, 3H); ^{13}C NMR (150 MHz, DMSO-d_6) δ 165.54, 162.04, 157.18, 154.19, 152.22, 151.04, 146.70, 144.75, 141.11, 137.48, 130.92, 127.70, 125.09, 120.35, 114.97, 113.88, 112.37, 109.49, 105.96, 102.26, 24.58; ^{19}F NMR (565 MHz, DMSO-d_6) δ -112.04; FT-IR (KBr, cm^{-1}): 1692.74 (stretch C=O), 1519.14 (bending N-H and stretch C-N), 3421.01 (stretch N-H); MS (ESI): *m/z* 388.4 $[M-H]^-$; HRMS (ESI): $C_{21}H_{17}O_2N_5F$ ($[M+H]^+$): calcd 390.1361, found 390.1353.

1-(4-Chlorophenyl)-3-(5-(2-methyl-4-oxo-4*H*-pyrido[1,2-*a*]pyrimidin-8-yl)pyridin-2-yl)urea (4g): yellowish solid; 89.6% yield; mp 263.2-266.7 °C; ^{1}H NMR (600 MHz, DMSO-d_6) δ 10.31 (s, 1H), 9.73 (s, 1H), 8.96 – 8.89 (m, 2H), 8.39 (dd, *J* = 8.8, 2.6 Hz, 1H), 7.98 (d, *J* = 2.1 Hz, 1H), 7.76 – 7.71 (m, 2H), 7.58 – 7.53 (m, 2H), 7.40 – 7.34 (m, 2H), 6.26 (s, 1H), 2.38 (s, 3H); ^{13}C NMR (150 MHz, DMSO-d_6) δ 165.60, 157.22, 154.29, 152.27, 151.10, 146.79, 144.87, 138.27, 137.58, 129.26, 127.76, 126.73, 125.13, 120.82, 120.42, 113.98, 112.38, 102.28, 24.61; FT-IR (KBr, cm^{-1}): 1682.17 (stretch C=O), 1558.56 (bending N-H and stretch C-N), 3431.12 (stretch N-H); MS (ESI): *m/z* 404.4 $[M-H]^-$; HRMS (ESI): $C_{21}H_{17}O_2N_5Cl$ ($[M+H]^+$): calcd 406.1065, found 406.1060.

1-(4-Fluorophenyl)-3-(5-(2-methyl-4-oxo-4*H*-pyrido[1,2-*a*]pyrimidin-8-yl)pyridin-2-yl)urea (4h): yellowish solid; 60.7% yield; mp 260.7-263.3 °C; ^{1}H NMR (600 MHz, DMSO-d_6) δ 10.23 (s, 1H), 9.69 (s, 1H), 8.92 – 8.89 (m, 2H), 8.36 (dd, *J* = 8.8, 2.6 Hz, 1H), 7.95 (d, *J* = 2.1 Hz, 1H), 7.73 – 7.69 (m, 2H), 7.53 (dd, *J* = 8.9, 4.9 Hz, 2H), 7.16 (t, *J* = 8.8 Hz, 2H), 6.24 (s, 1H), 2.36 (s, 3H); ^{13}C NMR (150 MHz, DMSO-d_6) δ 165.58, 157.48, 157.21, 154.41, 152.39, 151.08, 146.72, 144.85, 137.49, 135.59, 127.72, 124.96, 121.15, 121.10, 120.33, 116.00, 115.85, 113.94, 112.34, 102.26, 24.59; ^{19}F NMR (565 MHz, DMSO-d_6) δ -120.32; FT-IR (KBr, cm^{-1}): 1704.43 (stretch C=O), 1253.48 (stretch C-N and bending N-H), 3446.20 (stretch N-H); MS (ESI): *m/z* 388.3 $[M-H]^-$; HRMS (ESI): $C_{21}H_{17}O_2N_5F$ ($[M+H]^+$): calcd 390.1361, found 390.1355.

1-(5-(2-Methyl-4-oxo-4*H*-pyrido[1,2-*a*]pyrimidin-8-yl)pyridin-2-yl)-3-(4-(trifluoromethyl)phenyl)-urea (4i): yellowish solid; 63.0% yield; mp >270 °C; ^{1}H NMR (600 MHz, DMSO-d_6) δ 10.47 (s, 1H), 9.77 (s, 1H), 8.91 (d, *J* = 2.5 Hz, 2H), 8.38 (dd, *J* = 8.8, 2.4 Hz, 1H), 7.96 (s, 1H), 7.76 – 7.71 (m, 4H), 7.67 (d, *J* = 8.5 Hz, 2H), 6.24 (s, 1H), 2.36 (s, 3H); ^{13}C NMR (150 MHz, DMSO-d_6) δ 164.86, 156.49, 153.41, 151.49, 150.36, 146.11, 144.07, 142.31, 136.88, 127.03, 125.97, 125.12, 124.59, 123.32, 122.48, 122.27, 119.74, 118.26, 113.23, 111.73, 101.59, 23.89; ^{19}F NMR (565 MHz, DMSO-d_6) δ -60.18; FT-IR

(KBr, cm^{-1}): 1693.04 (stretch C=O), 1519.80 (bending N-H and stretch C-N), 3440.44 (stretch N-H); MS (ESI): *m/z* 438.4 $[M-H]^-$; HRMS (ESI): $C_{22}H_{17}O_2N_5F_3$ ($[M+H]^+$): calcd 440.1330, found 440.1321.

1-(2-Methoxyphenyl)-3-(5-(2-methyl-4-oxo-4*H*-pyrido[1,2-*a*]pyrimidin-8-yl)pyridin-2-yl)urea (4j): yellowish solid; 65.8% yield; mp >270 ℃; ^{1}H NMR (600 MHz, DMSO-d_6) δ 10.92 (s, 1H), 10.12 (s, 1H), 8.92 (d, *J* = 7.1 Hz, 2H), 8.37 – 8.35 (m, 1H), 8.20 (dd, *J* = 8.0, 1.6 Hz, 1H), 8.02 (d, *J* = 1.8 Hz, 1H), 7.78 (dd, *J* = 7.6, 2.1 Hz, 1H), 7.50 (s, 1H), 7.04 (d, *J* = 1.5 Hz, 1H), 7.01 (dd, *J* = 7.4, 1.7 Hz, 1H), 6.92 (dd, *J* = 7.7, 1.5 Hz, 1H), 6.26 (s, 1H), 3.96 (s, 3H), 2.37 (s, 3H); ^{13}C NMR (150 MHz, DMSO-d_6) δ 165.55, 157.21, 154.53, 152.30, 151.08, 148.58, 146.29, 144.80, 137.47, 128.70, 127.59, 124.72, 123.07, 121.01, 120.35, 119.21, 114.01, 112.40, 111.26, 102.23, 56.45, 24.57; FT-IR (KBr, cm^{-1}): 1687.27 (stretch C=O), 1514.64 (bending N-H and stretch C-N), 1254.60 (stretch -O-CH_3 Ar.), 3378.34 (stretch N-H); MS (ESI): *m/z* 424.1 $[M+Na]^+$; HRMS (ESI): $C_{22}H_{20}O_3N_5$ ($[M+H]^+$): calcd 402.1561, found 402.1553.

1-(5-(2-Methyl-4-oxo-4*H*-pyrido[1,2-*a*]pyrimidin-8-yl)pyridin-2-yl)-3-(2-(trifluoromethyl)phenyl)-urea (4k): yellowish solid; 54.2% yield; mp >270 ℃; ^{1}H NMR (600 MHz, DMSO-d_6) δ 11.34 (s, 1H), 10.32 (s, 1H), 8.90 (d, *J* = 7.4 Hz, 1H), 8.81 (d, *J* = 2.5 Hz, 1H), 8.39 (dd, *J* = 8.8, 2.6 Hz, 1H), 8.16 (d, *J* = 8.3 Hz, 1H), 7.98 (d, *J* = 2.1 Hz, 1H), 7.75 (dd, *J* = 7.5, 2.1 Hz, 1H), 7.72 (d, *J* = 7.9 Hz, 1H), 7.66 (d, *J* = 8.1 Hz, 1H), 7.39 (d, *J* = 6.5 Hz, 1H), 7.30 (t, *J* = 7.6 Hz, 1H), 6.25 (s, 1H), 2.36 (s, 3H); ^{13}C NMR (150 MHz, DMSO-d_6) δ 165.11, 156.76, 153.79, 152.14, 150.61, 145.16, 144.15, 137.48, 135.85, 133.13, 127.25, 126.02, 125.98, 124.79, 124.69, 123.92, 123.15, 120.18, 113.56, 112.20, 101.88, 24.14. ^{19}F NMR (565 MHz, DMSO-d_6) δ -60.37; FT-IR (KBr, cm^{-1}): 1693.42 (stretch C=O), 1520.52 (bending N-H and stretch C-N), 3420.62 (stretch N-H); MS (ESI): *m/z* 462.3 $[M+Na]^+$; HRMS (ESI): $C_{22}H_{17}O_2N_5F_3$ ($[M+H]^+$): calcd 440.1330, found 440.1323.

1-(2-Fluorophenyl)-3-(5-(2-methyl-4-oxo-4*H*-pyrido[1,2-*a*]pyrimidin-8-yl)pyridin-2-yl)urea (4l): yellowish solid; 61.9% yield; mp >270 ℃; ^{1}H NMR (600 MHz, DMSO-d_6) δ 10.56 (s, 1H), 10.06 (s, 1H), 8.90 – 8.86 (m, 2H), 8.36 (dd, *J* = 8.8, 2.6 Hz, 1H), 8.22 – 8.18 (m, 1H), 7.96 (d, *J* = 2.0 Hz, 1H), 7.74 (dd, *J* = 7.5, 2.1 Hz, 1H), 7.62 (d, *J* = 8.8 Hz, 1H), 7.27 (dd, *J* = 11.4, 8.2 Hz, 1H), 7.16 (t, *J* = 7.8 Hz, 1H), 7.06 (dd, *J* = 7.4, 1.7 Hz, 1H), 6.23 (s, 1H), 2.36 (s, 3H); ^{13}C NMR (150 MHz, DMSO-d_6) δ 165.46, 157.16, 154.27, 153.43, 152.18, 151.82, 151.01, 146.45, 144.76, 137.59, 127.65, 127.29, 125.07, 123.70, 121.43, 120.37, 115.56, 113.97, 112.48, 102.27, 24.54; ^{19}F NMR (565 MHz, DMSO-d_6) δ -129.26; FT-IR (KBr, cm^{-1}): 1673.75 (stretch C=O), 1518.23 (bending N-H and stretch C-N), 3418.44 (stretch N-H); MS (ESI): *m/z* 388.0 $[M-H]^-$; HRMS (ESI): $C_{21}H_{17}O_2N_5F$ ($[M+H]^+$): calcd 390.1361, found 390.1355.

1-(2-Chlorophenyl)-3-(5-(2-methyl-4-oxo-4*H*-pyrido[1,2-*a*]pyrimidin-8-yl)pyridin-2-yl)urea (4m): yellowish solid; 73.2% yield; mp 254.5-258.9 ℃; ^{1}H NMR (600 MHz, DMSO-d_6) δ 11.56 (s, 1H), 10.29 (s, 1H), 8.94 (d, *J* = 2.5 Hz, 1H), 8.88 (d, *J* = 7.5 Hz, 1H), 8.37 (dd, *J* = 8.8, 2.6 Hz, 1H), 8.33 (dd, *J* = 8.3,

1.4 Hz, 1H), 8.00 (d, *J* = 2.1 Hz, 1H), 7.75 (dd, *J* = 7.5, 2.1 Hz, 1H), 7.49 (dd, *J* = 8.0, 1.5 Hz, 1H), 7.37 (d, *J* = 8.6 Hz, 1H), 7.33 – 7.30 (m, 1H), 7.06 (t, *J* = 7.6 Hz, 1H), 6.23 (s, 1H), 2.35 (s, 3H); ^{13}C NMR (150 MHz, DMSO-d_6) δ 165.52, 157.18, 154.19, 152.28, 151.04, 146.05, 144.57, 137.68, 136.35, 129.70, 128.07, 127.61, 124.86, 124.17, 122.64, 121.45, 120.44, 113.90, 112.52, 102.27, 24.57; FT-IR (KBr, cm^{-1}): 1641.44 (stretch C=O), 1557.25 (bending N-H and stretch C-N), 3422.94 (stretch N-H); MS (ESI): *m/z* 404.0 [M-H]$^-$; HRMS (ESI): $C_{21}H_{17}O_2N_5Cl$ ([M+H]$^+$): calcd 406.1065, found 406.1057.

1-(4-Bromophenyl)-3-(5-(2-methyl-4-oxo-4*H*-pyrido[1,2-*a*]pyrimidin-8-yl)pyridin-2-yl)urea (4n): yellowish solid; 52.8% yield; mp 265.5-269.7 °C; ^{1}H NMR (600 MHz, DMSO-d_6) δ 10.31 (s, 1H), 9.71 (s, 1H), 8.90 (d, *J* = 7.5 Hz, 1H), 8.88 (d, *J* = 2.5 Hz, 1H), 8.34 (dd, *J* = 8.8, 2.6 Hz, 1H), 7.93 (d, *J* = 2.2 Hz, 1H), 7.72 – 7.68 (m, 2H), 7.48 (s, 2H), 7.42 (d, *J* = 8.5 Hz, 2H), 6.24 (s, 1H), 2.36 (s, 3H); ^{13}C NMR (150 MHz, DMSO-d_6) δ 165.23, 156.86, 153.87, 151.84, 150.68, 146.32, 144.44, 139.01, 138.29, 137.13, 131.68, 127.35, 124.70, 120.82, 120.37, 119.96, 114.30, 113.55, 112.01, 101.91, 24.22; FT-IR (KBr, cm^{-1}): 1634.27 (stretch C=O), 1557.02 (bending N-H and stretch C-N), 3418.17 (stretch N-H); MS (ESI): *m/z* 448.0 [M-H]$^-$; HRMS (ESI): $C_{21}H_{17}O_2N_5Br$ ([M+H]$^+$): calcd 450.0560, found 450.0554.

General procedure for the preparation of 10. *N*-(5-(2-Methyl-4-oxo-4*H*-pyrido[1,2-*a*]-pyrimidin-8-yl)-1*H*-benzo[*d*]imidazol-2-yl)butyramide (10a). First, intermediates **7**, **8**, and **9** were sequentially prepared according to previously reported well-established methods using 4-bromo-2-nitroaniline and intermediate **2** synthesized in Scheme 1 as the raw material and Scheme 2 as the synthetic route.[15] Among them, we prepared intermediate **6** by the previously reported method using 4-bromo-2-nitroaniline as the raw material.[11] Then, **9** (0.25 g, 0.85 mmol) and Et_3N (0.17 g, 1.70 mmol) were added to 20 mL of DCM and stirred for 5 min. Subsequently, a solution of butyryl chloride (0.14 g, 1.3 mmol) was added dropwise to the reaction mixture using a dropping funnel under ice-cold conditions, and after the drop was completed, the reaction was stirred with time for about 1 h at room temperature. The completion of the reaction was monitored by TLC. After the reaction was completed, the reaction solution was added to 50 mL of saturated aqueous $NaHCO_3$ solution, extracted three times with DCM (50 mL×3), the organic phase was dried over $MgSO_4$, and the solvent was removed by concentration under reduced pressure, and the residue obtained was purified by DCM/MeOH column chromatography on silica gel to give **10a**.

8-(4-Amino-3-nitrophenyl)-2-methyl-4*H*-pyrido[1,2-*a*]pyrimidin-4-one (7): yellow solid; 69.1% yield. ^{1}H NMR (600 MHz, DMSO-d_6) δ 8.84 (d, *J* = 7.5 Hz, 1H), 8.47 (d, *J* = 2.3 Hz, 1H), 8.02 (dd, *J* = 9.0, 2.3 Hz, 1H), 7.83 (s, 2H), 7.80 (d, *J* = 2.1 Hz, 1H), 7.66 (dd, *J* = 7.6, 2.1 Hz, 1H), 7.12 (d, *J* = 8.9 Hz, 1H), 6.19 (s, 1H), 2.34 (s, 3H); ^{13}C NMR (150 MHz, DMSO-d_6) δ 165.23, 156.87, 150.79, 147.24, 145.53, 133.76, 130.48, 127.21, 124.48, 121.77, 120.41, 118.89, 113.46, 101.57, 24.23. FT-IR (KBr, cm^{-1}):

1523.73 (stretch Ar-NO_2), 3323.56, 3477.07 (stretch -NH_2 Ar.), 1693.03 (stretch C=O); MS (ESI): *m/z* 296.09, 295.0 $[M-H]^-$. HRMS (ESI): $C_{15}H_{13}O_3N_4$ ($[M+H]^+$): calcd 297.0982, found 297.0976.

8-(3,4-Diaminophenyl)-2-methyl-4*H*-pyrido[1,2-*a*]pyrimidin-4-one (8): yellow solid; 73.6% yield; ^{1}H NMR (600 MHz, DMSO-d_6) δ 8.82 (d, *J* = 7.5 Hz, 1H), 7.58 (d, *J* = 2.1 Hz, 1H), 7.55 (dd, *J* = 7.6, 2.2 Hz, 1H), 7.14 (d, *J* = 2.2 Hz, 1H), 7.10 (dd, *J* = 8.1, 2.3 Hz, 1H), 6.63 (d, *J* = 8.1 Hz, 1H), 6.13 (s, 1H), 4.99 (s, 4H), 2.33 (s, 3H); ^{13}C NMR (150 MHz, DMSO-d_6) δ 165.13, 156.98, 151.03, 148.49, 138.82, 135.15, 126.73, 122.68, 117.63, 116.52, 114.24, 113.89, 112.29, 100.55, 24.26. FT-IR (KBr, cm^{-1}): 3405.98 (stretch -NH_2 Ar.), 1693.26 (stretch C=O); MS (ESI): *m/z* 266.12, 265.0 $[M-H]^-$. HRMS (ESI): $C_{15}H_{15}N_4O$ ($[M+H]^+$): calcd 267.1240, found 267.1230.

8-(2-Amino-1*H*-benzo[*d*]imidazol-5-yl)-2-methyl-4*H*-pyrido[1,2-*a*]pyrimidin-4-one (9): yellow solid; 67.8% yield; ^{1}H NMR (600 MHz, DMSO-d_6) δ 10.97 (s, 1H), 8.88 (d, *J* = 7.5 Hz, 1H), 7.79 (d, *J* = 2.1 Hz, 1H), 7.71 (dd, *J* = 7.5, 2.1 Hz, 1H), 7.68 (d, *J* = 1.9 Hz, 1H), 7.51 (d, *J* = 8.2 Hz, 1H), 7.24 (d, *J* = 8.2 Hz, 1H), 6.47 (s, 2H), 6.19 (s, 1H), 2.35 (s, 3H); ^{13}C NMR (150 MHz, DMSO-d_6) δ 165.55, 157.36, 157.29, 151.23, 149.53, 127.20, 126.20, 119.65, 119.01, 115.03, 101.39, 24.57; ^{13}C NMR (150 MHz, DMSO-d_6) δ 165.55, 157.36, 157.29, 151.23, 149.53, 127.20, 126.20, 119.65, 119.01, 115.03, 101.39, 24.57; FT-IR (KBr, cm^{-1}): 3382.55 (stretch N-H), 1636.01 (stretch C=O); MS (ESI): *m/z* 291.11, 290.0 $[M-H]^-$. HRMS (ESI): $C_{16}H_{14}N_5O$ ($[M+H]^+$): calcd 292.1193, found 292.1182.

***N*-(5-(2-Methyl-4-oxo-4*H*-pyrido[1,2-*a*]pyrimidin-8-yl)-1*H*-benzo[*d*]imidazol-2-yl)butyramide (10a):** yellowish solid; 30.2% yield; mp >270 °C; ^{1}H NMR (600 MHz, DMSO-d_6) δ 12.30 (s, 1H), 11.63 (s, 1H), 8.93 (s, 1H), 8.00 (d, *J* = 7.8 Hz, 1H), 7.90 – 7.67 (m, 3H), 7.63 – 7.54 (m, 1H), 6.23 (s, 1H), 2.44 (t, *J* = 7.3 Hz, 2H), 2.37 (s, 3H), 1.69 – 1.63 (m, 2H), 0.94 (t, *J* = 7.4 Hz, 3H). ^{13}C NMR (150 MHz, DMSO-d_6) δ 173.25, 165.62, 158.79, 157.33, 151.32, 149.32, 130.50, 127.49, 120.22, 115.16, 101.71, 40.71, 37.93, 24.59, 18.62, 13.86; FT-IR (KBr, cm^{-1}): 1646.19 (stretch C=O), 1309.32 (stretch C-N and bending N-H), 1646.19 (stretch C=O); MS (ESI): *m/z* 384.4 $[M+Na]^+$; HRMS (ESI): $C_{20}H_{20}O_2N_5$ ($[M+H]^+$): calcd 362.1612, found 362.1620.

***O*-(5-(2-Methyl-4-oxo-4*H*-pyrido[1,2-*a*]pyrimidin-8-yl)-1*H*-benzo[*d*]imidazol-2-yl)pivalamide (10b):** yellowish solid; 31.8% yield; mp 267.0-268.5 °C; The purity value measured by HPLC was 99.80%; ^{1}H NMR (600 MHz, DMSO-d_6) δ 12.35 (s, 1H), 11.29 (s, 1H), 8.92 (d, *J* = 7.5 Hz, 1H), 8.01 (s, 1H), 7.93 – 7.64 (m, 3H), 7.58 (s, 1H), 6.22 (s, 1H), 2.37 (s, 3H), 1.29 (s, 9H); ^{13}C NMR (150 MHz, DMSO-d_6) δ 178.48, 165.56, 157.26, 151.23, 149.13, 141.82, 134.90, 127.44, 121.41, 120.76, 120.17, 117.95, 116.28, 115.13, 112.65, 110.60, 101.77, 27.09, 24.64; FT-IR (KBr, cm^{-1}): 1632.99, 1670.97 (stretch C=O), 3394.88 (stretch N-H), 1171.25 (stretch C-N); MS (ESI): *m/z* 374.1 $[M-H]^-$; HRMS (ESI): $C_{21}H_{22}O_2N_5$ ($[M+H]^+$): calcd 376.1768, found 376.1778.

4-(*tert*-Butyl)-*N*-(5-(2-methyl-4-oxo-4*H*-pyrido[1,2-*a*]pyrimidin-8-yl)-1*H*-benzo[*d*]imidazol-2-yl)-benzamide (10c): yellowish solid; 25.9% yield; mp >270 ℃; ^{1}H NMR (600 MHz, DMSO-d_6) δ 12.44 (s, 2H), 8.94 (d, *J* = 7.4 Hz, 1H), 8.09 (d, *J* = 8.2 Hz, 2H), 8.04 (d, *J* = 1.8 Hz, 1H), 7.88 (s, 1H), 7.76 (dd, *J* = 8.3, 1.9 Hz, 2H), 7.63 (d, *J* = 8.3 Hz, 1H), 7.57 (d, *J* = 8.2 Hz, 2H), 6.24 (s, 1H), 2.38 (s, 3H), 1.32 (s, 9H); ^{13}C NMR (150 MHz, DMSO-d_6) δ 181.03, 167.26, 165.60, 157.28, 156.01, 151.21, 149.60, 149.03, 137.88, 130.77, 128.93, 128.65, 127.53, 125.83, 121.38, 120.23, 115.14, 110.39, 101.83, 35.26, 31.33, 24.63; FT-IR (KBr, cm^{-1}): 1635.23, 1670.68 (stretch C=O), 3397.91 (stretch N-H), 1272.27 (stretch C-N); MS (ESI): *m/z* 450.1 [M-H]$^-$; HRMS (ESI): $C_{27}H_{25}O_2NaN_5$ ([M+Na]$^+$): calcd 474.1887, found 474.1891.

Molecular modeling. Molecular docking simulations were performed using Molecular Operating Environment (MOE, Version 2020).[16] ROR1 (PDB code 6TU9) was selected for the docking study and its crystal structure was obtained from the RSCB PDB database. The protein was optimized and energy minimized using the default parameters of MOE. Docking points were defined by the Site Finder program. The docking results were analyzed using Accelrys Discovery Studio Visualizer 4.5.

Cell viability assay. Cell viability was determined using the MTT assay. Briefly, cells were inoculated into 96-well plates and treated with different concentrations of compounds for 72 h. The number of viable cells was detected by flow cytometry, and the data were analyzed using SPSS software to calculate the IC_{50} value for each product.

Cell cycle assay. Cell cycle assays were performed using propidium iodide (PI) staining. Tumor cells were inoculated in 6-well plates and then compound **10b** was added to treat the cells for 48 h, after which the cells were collected and fixed in 70% ice-cold EtOH. Cells were stained with PI staining buffer. All samples were processed according to the manufacturer's protocol. Finally, assays were performed by flow cytometry.

Cell apoptosis assay. Apoptosis was detected using Annexin V- FITC/PI double staining, as described previously.[15] Briefly, tumor cells H1975 were inoculated overnight, after which the cells were treated with compound **10b** for 48 h and stained with Annexin V and PI. Finally, flow cytometry analysis was performed according to the manufacturer's protocol.

Western blot. Cells were treated with different concentrations of compound **10b**. Western blot analysis was performed as described previously.[17] Blots were imaged with a ChemiDoc™ MP imaging system (Bio-Rad, USA). All bands were analyzed using Image J software.

ACKNOWLEDGEMENTS

This work was supported by the Natural Science Foundation of Guizhou Provincial Science and Technology Projects (grant number QKH-zk [2022] 030); The Science and Technology Plan Project of Guizhou Province, China (QKHPTRC[2018]5779-59); Merit-based Funding Program for Innovation and

Entrepreneurship of High-level Overseas Talents of Guizhou Province (Grant No. 202001) and National Natural Science Foundation of China (Grants 22167010).

REFERENCES

1. R. L. Siegel, K. D. Miller, and A. Jemal, *CA. Cancer J. Clin.*, 2018, **68**, 7.
2. (a) R. S. Herbst, D. Morgensztern, and C. Boshoff, *Nature.*, 2018, **553**, 446; (b) H. Sung, J. Ferlay, R. L. Siegel, M. Laversanne, I. Soerjomataram, A. Jemal, and F. Bray, *CA. Cancer J. Clin.*, 2021, **71**, 209.
3. (a) A. C. Gelatti, A. Drilon, and F. C. Santini, *Lung Cancer*, 2019, **137**, 113; (b) L. C. Chang, C. K. Lim, L. Y. Chang, K. Y. Chen, J. Y. Shih, and C. J. Yu, *Eur. J. Cancer*, 2019, **119**, 77.
4. (a) Y. Jia, C. H. Yun, E. Park, D. Ercan, M. Manuia, J. Juarez, C. Xu, K. Rhee, T. Chen, and H. Zhang, *Nature*, 2016, **534**, 129; (b) C. Jin and P. Yuan, *Oncol. Lett.*, 2020, **20**, 2091.
5. (a) C. L. Chiang, S. Goswami, F. W. Frissora, Z. Xie, P. S. Yan, R. Bundschuh, L. A. Walker, X. Huang, R. Mani, and X. M. Mo, *Blood*, 2019, **134**, 432; (b) S. Zhang, L. Chen, B. Cui, H. Y. Chuang, J. Yu, J. Wang-Rodriguez, L. Tang, G. Chen, G. W. Basak, and T. J. Kipps, *PLOS ONE.*, 2012, **7**, e31127; (c) S. Zhang, B. Cui, H. Lai, G. Liu, E. M. Ghia, G. F. Widhopf, Z. Zhang, C. C. Wu, L. Chen, and R. Wu, *Proc. Natl. Acad. Sci. USA*, 2014, **111**, 17266; (d) Y. Zhao, D. Zhang, Y. Guo, B. Lu, Z. J. Zhao, X. Xu, and Y. Chen, *Front. Oncol.*, 2021, **11**, 680834.
6. A. Gentile, L. Lazzari, S. Benvenuti, L. Trusolino, and P. M. Comoglio, *Cancer Res.*, 2011, **71**, 3132.
7. M. Hojjat-Farsangi, A. S. Khan, A. H. Daneshmanesh, A. Moshfegh, Å. Sandin, L. Mansouri, M. Palma, J. Lundin, A. Österborg, and H. Mellstedt, *PLOS ONE.*, 2013, **8**, e78339.
8. (a) S. Saengchantara and T. Wallace, *Nat. Prod. Rep.*, 1986, **3**, 465; (b) Y. Y. Jiang, F. X. Guo, L. X. Chen, L. L. Xu, W. Zhang, and B. Liu, *Fitoterapia*, 2019, **135**, 114; (c) S. K. Roy, N. Kumari, S. Gupta, S. Pahwa, H. Nandanwar, and S. M. Jachak, *Eur. J. Med. Chem.*, 2013, **66**, 499; (d) S. Noushini, E. Alipour, S. Emami, M. Safavi, S. K. Ardestani, A. R. Gohari, A. Shafiee, and A. Foroumadi, *DARU*, 2013, **21**, 1.
9. X. S. Liu, W. C. Pu, H. Y. He, X. Fan, Y. Y. Zheng, J. K. Zhou, R. Ma, J. He, Y. Z. Zheng, and K. Wu, *Cancer Lett.*, 2019, **458**, 76.
10. P. Sikka, J. Sahu, A. Mishra, and S. Hashim, *Med. Chem.*, 2015, **5**, 479.
11. C. Fan, T. Zhong, H. Yang, Y. Yang, D. Wang, X. Yang, Y. Xu, and Y. Fan, *Eur. J. Med. Chem.*, 2020, **190**, 112108.
12. L. Peng, X. Gao, L. Duan, X. Ren, D. Wu, and K. Ding, *J. Med. Chem.*, 2011, **54**, 7729.
13. Z. Dave, O. Vondálová Blanářová, Š. Čada, P. Janovská, N. Zezula, M. Běhal, K. Hanáková, S. R. Ganji, P. Krejci, and K. Gömöryová, *Front. Cell Dev. Biol.*, 2022, **10**, 838871.

14. T. Yamaguchi, K. Yanagisawa, R. Sugiyama, Y. Hosono, Y. Shimada, C. Arima, S. Kato, S. Tomida, M. Suzuki, and H. Osada, *Cancer Cell*, 2012, **21**, 348.
15. Y. Fan, F. Luo, M. Su, Q. Li, T. Zhong, L. Xiong, M. Li, M. Yuan, and D. Wang, *Bioorg. Chem.*, 2023, **132**, 106352.
16. H. Yang, Q. Li, M. Su, F. Luo, Y. Liu, D. Wang, and Y. Fan, *Bioorg. Med. Chem.*, 2021, **46**, 116346.
17. A. Lodola, S. Bertolini, M. Biagetti, S. Capacchi, F. Facchinetti, P. M. Gallo, A. Pappani, M. Mor, D. Pala, and S. Rivara, *J. Med. Chem.*, 2017, **60**, 4304.